Journal of Earth Sciences and Geotechnical Engineering, vol. 3, no. 4, 2013, 107-123
ISSN: 1792-9040 (print), 1792-9660 (online)
Scienpress Ltd, 2013

Imaging the Subsurface in the Cameroon Centre Region using the Audio-magnetotellurics (AMT) Soundings for the Monitoring of the Monatele-sa'a Earthquake Area

T. Ndougsa-Mbarga[1], D.H. Gouet[2], D. Bisso[3], A. Meying[4], and E. Manguele-Dicoum[5]

Abstract

In monitoring the Monatélé-Sa'a earthquake area, audiomagnetotelluric investigation was carried out using a scalar instrument with a frequency range from 4.1 Hz to 2300 Hz. Data have been collected in the Ntui-Sa'a area near Monatélé, along a profile containing seven (07) stations directed N-S, covering approximately a distance of 16.5 km. This profile crosses the Sanaga River which seems to be parallel to a buried big fault which shows no indication on the surface. The validation of the measured resistivity and calculated phase data set is done by the application of dimensionality. The interpretation of data using 2D inversion imaging of the subsurface has lead to the confirmation of two major discontinuities:

- The Sanaga fault oriented SSW-NNE, covered by a thick layer of alluvial deposit in the Elang III area. This fault is bisected to a lateral fracture between Nkolessono and Elang III.
- The fault network in Biakoa-Goura intersected the Sanaga fault is characterised by secondary faults in Biakoa and Talba.

The presence of a fault network traversing the Sanaga fault shows that the study area belongs to the major tectonic accident area known as the Cameroon Central shear zone (CCSZ). The tectonic node relaxation of the Biakoa-Goura seems to be the origin of the February 2005 earthquake in Monatélé and Yaoundé northern areas.

[1]Department of Physics, Advanced Teacher's Training College, University of Yaoundé I, P.O. Box 47, Yaoundé Cameroon
[2]Department of Physics, Faculty of Science, University of Yaoundé I, P.O. Box 812, Yaoundé Cameroon.
[3]Department of Earth Sciences, Faculty of Science, University of Yaoundé I, P.O. Box 812, Yaoundé Cameroon.
[4] Geology and Mining Exploitation School, University of Ngaounderé, P.O. Box 454, Ngaounderé, Cameroon.
[5] Department of Physics, Faculty of Science, University of Yaoundé I, P.O. Box 812, Yaoundé Cameroon.

The interpretation revealed that quartzite, gneiss and migmatite are in discordance on a basement composed of granite.

Keywords: AMT soundings, dimensionality, resistivity, phase, 2D inversion, fault, tectonic node, Monatélé-Sa'a, Cameroon.

1 Introduction

The Sanaga fault had been put in evidence by Dumont (1986) and confirmed by Bisso et al (2004) respectively based on remote sensing and audiomagnetotellurics (AMT) analyses. These studies showed that the Sanaga fault seems to follow the course of Sanaga River by Ebebda and bisects to a fault network which in fact heads towards Ntui-Sa'a (Bisso et al, 2004; Dumont, 1986). To know the impact of this fault, it is important to highlight that the region has been subjected to a low magnitude earthquake recently in February 2005. This study has as objective, the collection of data along a profile which would have to permit after interpretations, to tell if this fault network which is bisected to the Sanaga fault belongs to the Cameroon Central shear zone of the Pan African belt or probably to a local tectonic accident network (Cornachia and Dars, 1983).
An audiomagnetotelluric (AMT) prospecting and the exploitation of data collected along one profile having seven (07) sounding stations (Fig. 1, Table 1) based on the combination of the magnetotelluric method (Cagniard, 1953; Vozoff, 1972 and 1990) and the MT inversion (Parker and Booker, 1996) as well as their interpretations have permitted us to image the subsurface of the Monatélé-Sa'a region, particularly the Sa'a area. The study area (Fig. 1) is situated in the northern part of Yaoundé (Fig. 2a) of the Cameroon central domain (Mvondo et al, 2007a) between latitudes 4°N and 5°N, and longitudes 11°E and 12°E.

Table 1: Positions and names of stations

Stations (A_i)	Longitude (x)	Latitude (y)	Altitude (z)	Distance (km)
A_1 NKOLESSONO	11°28,979'	04°25,722'	480	0
A_2 ELANG III	11°29,458'	04°26'	465	3
A_3 KORA	11°29,095'	04°29,038'	445	5
A_4 BINDAMONGO	11°29,715'	04°30,972'	480	9
A_5 BIAKOA	11°29,433'	04°32,370'	475	12
A_6 C. KEMAYO	11°28,084'	04°34,370'	500	14
A_7 TALBA	11°28,407'	04°34,779'	505	16,5

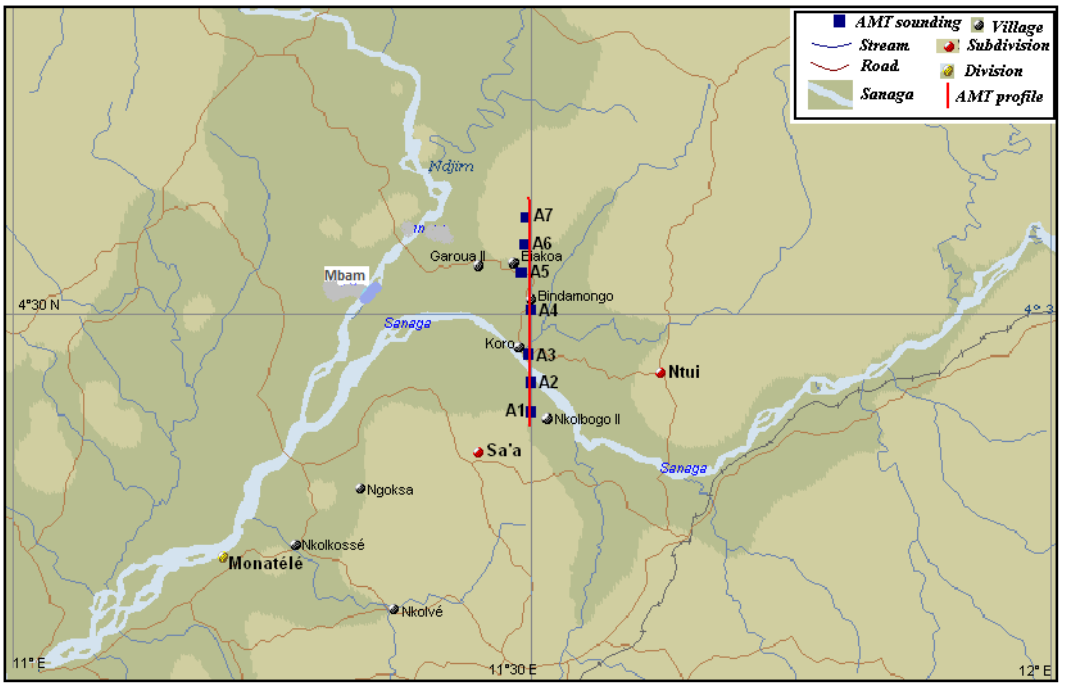

Figure 1: Localization map of sounding stations

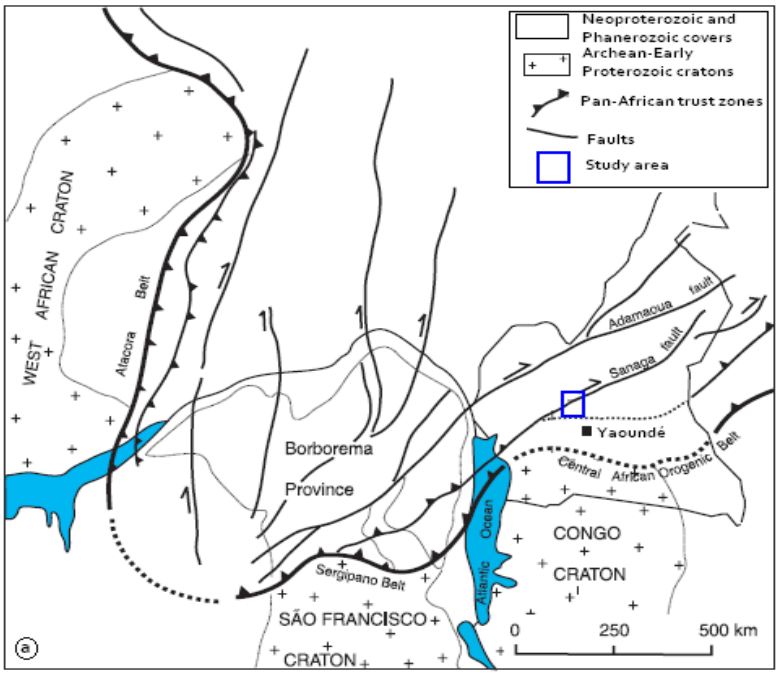

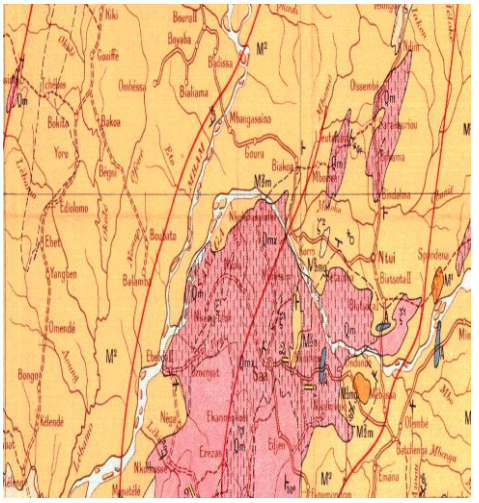

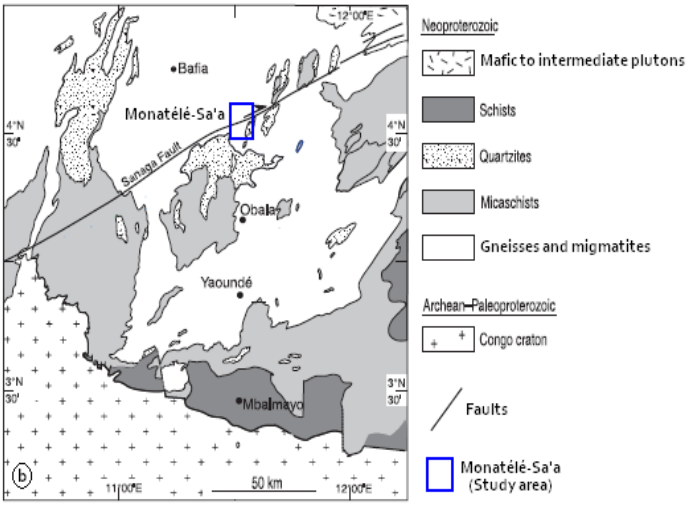

Figure 2: (a) Tectonic map of the study area location (modified from Mvondo *et al* 2007a). (b) Structural map of the Central African Fault Zone (modified from Mvondo *et al* 2007a). (c)Geological map of the study area (after Gazel and Hourcq, 1964)

2 Tectonic and Geological Setting

The Monatélé-Sa'a area belongs to the central Cameroon domain and is located between latitudes 4°N and 5° N and longitudes 11°E and 12°E .The study area (Fig. 1) presents an equatorial climate type. The humidity and temperature vary less. The Sanaga river is the principal hydrographical collector of the region. The topography is relatively the same, with an average altitude which ranges between 400 m to 600 m. The vegetation is that of the dense forest.

A greater part of Cameroon is made up of a Precambrian basement including magmatic and metamorphic rocks belonging to different geological periods. These rocks are

constituted of granite, gneiss and migmatite, renovated during the Pan African episode (Meying et al, 2009). The Monatélé-Sa'a area, found in the middle part of the north Equatorial Pan African belt, is an integral part of the Yaoundé series which is constituted essentially of granulites, migmatites and medium grade schists (Bisso et al, 2004). The protolithes correspond to a platform of marly sedimentary series with basic volcanic interstratified levels (Bisso et al, 2004). This neoproterozoic series was subject to a triphase tectonic associated to migmatization (Bisso et al, 2004; Mvondo et al, 2007a):
- a D1 phase represented by isoclinally folded and second axial planar foliation.
- a D2 tangential phase characterised by differential displacement and folds linked to a continental collision metamorphic micaschites, gneiss, migmatites and granites of the Mobile zone (Bisso et al, 2004; Nzenti et al, 1999).
- a D3 brittle phase which corresponds to mylonitic shears and faulting.

The conditions of paroxysmal metamorphism were estimated at 800°C and 10-12Kb (Bisso et al, 2004). The granulitic metamorphism is dated at 620 ± 10 Ma (Penaye et al, 1993)

The geological observations based on rock lithology on one hand and tectonic facts on the other hand, show that the Monatélé-Sa'a area belongs to the Pan-African cycle.

3 Audiomagnetotelluric Data

The data acquisition was based on the principle of the magnetotelluric (MT) method (Cagniard, 195; Vozoff 1972 and 1990) using the resistivity-meter ECA 540-0 which measured simultaneously the electric and magnetic field components Ex and Hy respectively of the natural wave (Manguelle-Dicoum et al, 1992 and 1993; Bisso et al, 2004; Meying et al, 2009). The AMT data are collected following the telluric lines E-W & S-N. The sounding curves following the telluric lines E-W & S-N (Fig. 3a-b) using the MT Inversion (Parker and Booker, 1996) show that the line SN is the longitudinal direction to the structure and the line EW is the transversal direction to the structure (Swift, 1967). The resistivity meter measures the apparent resistivity $\rho_{a\perp}$ following the E-W telluric line and the apparent resistivity ρ_α following the S-N telluric line (Manguelle-Dicoum et al, 1992). At each frequency and following a direction, five (05) resistivity values are collected. The obtained data of each frequency and direction permitted the calculation of the weighted arithmetic mean $\rho_{a\perp}$ and ρ_α. Then the apparent phases (Phi) of telluric lines E-W ($\phi_{a\perp}$) and SN (Φ_α) following the Bostick transformation defined by the relation $\phi_a = \frac{\prod}{4}\left(1+\frac{F\Delta\rho_a}{\rho_a \Delta F}\right)$ where F, ρ_a, ΔF, $\Delta\rho_a$ and ϕ_a are respectively the frequency, the apparent resistivity, the variation of the frequency, the variation of the apparent resistivity and the apparent phase or Phi (Bostick, 1977). The phase calculated following the Bostick transformation must be in the range 0-90° required by any one dimensional response (Parker and Booker, 1996).

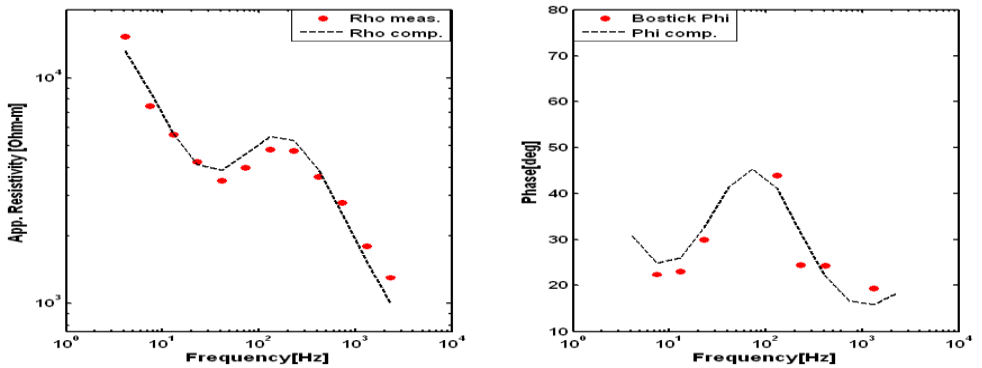

a)-Sounding curves of the MT inversion with Rhoplus of Rho measured and Phi calculed (Bostick, 1977) of the station A7 following telluric line EW

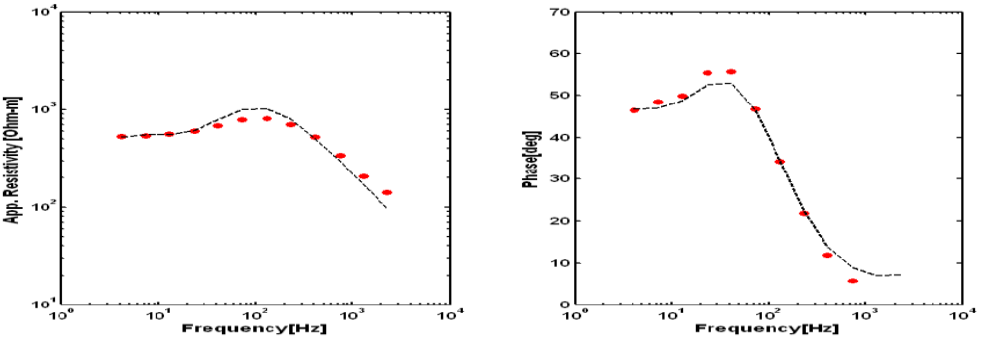

b)-Sounding curves of the MT inversion with Rhoplus of Rho measured and Phi calculed (Bostick, 1977) of the station A7 following telluric line SN

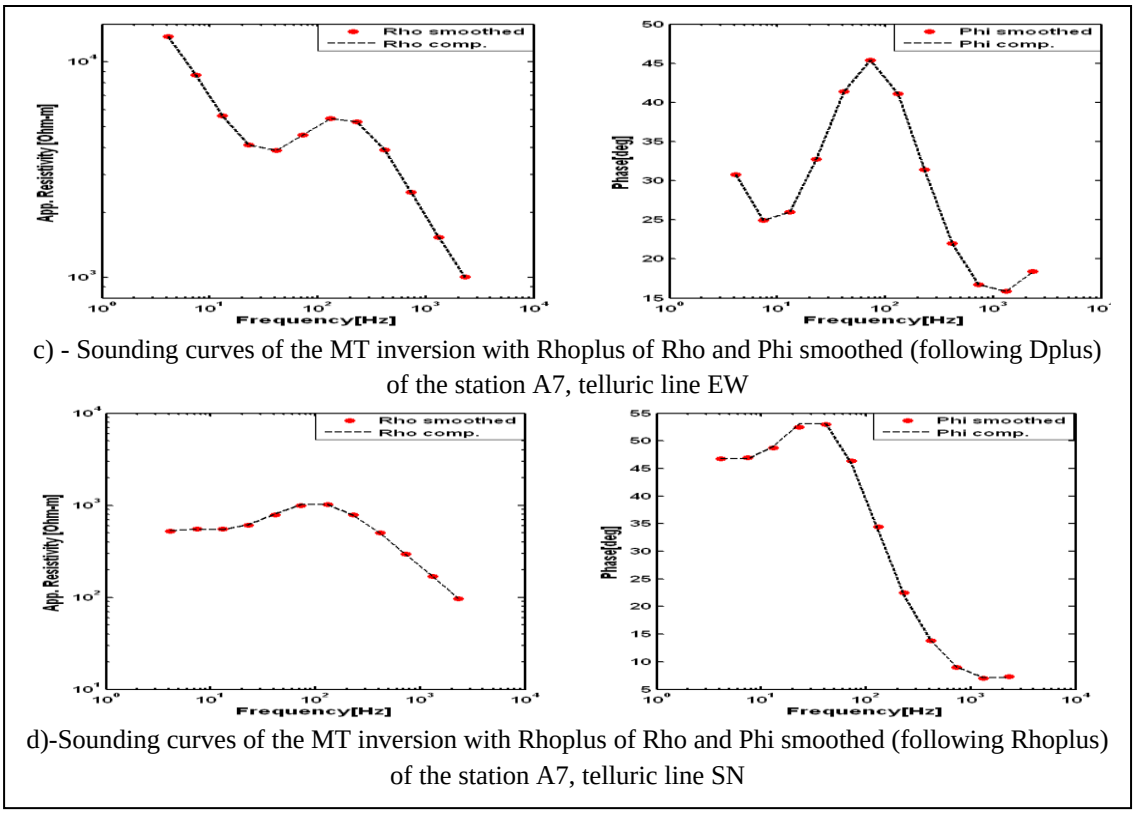

c) - Sounding curves of the MT inversion with Rhoplus of Rho and Phi smoothed (following Dplus) of the station A7, telluric line EW

d)-Sounding curves of the MT inversion with Rhoplus of Rho and Phi smoothed (following Rhoplus) of the station A7, telluric line SN

Figure 3: (a-b) AMT sounding curves of the MT Inversion with Rhoplus of measured and calculed data (Parker and Booker 1996).
(c-d) AMT sounding curves of the MT Inversion with Rhoplus of smoothed data following Rhoplus (Parker and Booker 1996).

4 Methodology

4.1 Validation of Resistivity and Phase Data

The collected AMT data were generally influenced by the disruptive sources (Fig. 3a-b) (Jones, 1988). Indeed, regional currents induced by natural sources can be problematic in certain situations, and the appropriate interpretational dimensionality must be known (Jones and Garcia, 2003). Our study being regional on one wide AMT profile, the 3D interpretation is not valid (Jones and Garcia, 2003). The dimensionality of data measured using the MT inversion (Parker and Booker, 1996) permits on the one hand to determine if the appropriate interpretational dimension must be in 1D or 2D, or in 1D and 2D, and the other hand to validate the analytical AMT data (analytical ρ_a and analytical ϕ_a) across a robust smoothing AMT data measured (ρ_a measured) and calculated (Bostick phase ϕ_a) following the MT inversion (Parker and Booker, 1996; Bostick, 1977).
The sounding curves (fig. 3(a)-(b)) of measured resistivity ($\rho_{a\perp}$ & ρ_a) and calculated phase following Bostick transformation ($\phi_{a\perp}$ & ϕ_a) of telluric EW & SN lines show that most

data exceeds the 95% confidence limit of computed values (Parker and Booker, 1996). This dispersion of the resistivity and phase data set shows that the regional effect is not negligible and the 1D interpretation is not appropriate. Thus, the appropriate interpretational dimension is 2D. However, the appropriate data for a 1D, 2D or 3D interpretation must be included in the 95% confidence limit in relation data with computed values (Parker and Booker, 1996). In this effect, a robust smoothing using MT inversion with Rhoplus permits to bring back the measured resistivity AMT data and calculated phase following the telluric lines EW & SN in the 95% confidence limit (Jones and Garcia, 2003; Parker and Booker, 1996). The smoothed data set following the telluric line EW & SN (Figure 3(c)-(d)) permits to have analytical resistivity ρ_a and phase ϕ_a following the relations $\rho_a = \sqrt{(\rho_{a\perp} \times \rho_{a\parallel})}$ and $\phi_a = \sqrt{(\phi_{a\perp} \times \phi_{a\parallel})}$ respectively (Jones and Garcia, 2003; Parker and Booker, 1996; Guérin et al, 1994). The analytic data illustrated by sounding curves (Fig. 4) following the inversion procedure with Rhoplus (Parker and Booker, 1996) are used in the profiling curves, apparent resistivity pseudosections, apparent phase pseudosections and the 2-D resistivity models (Fig. 5, 6, 7 and 8).

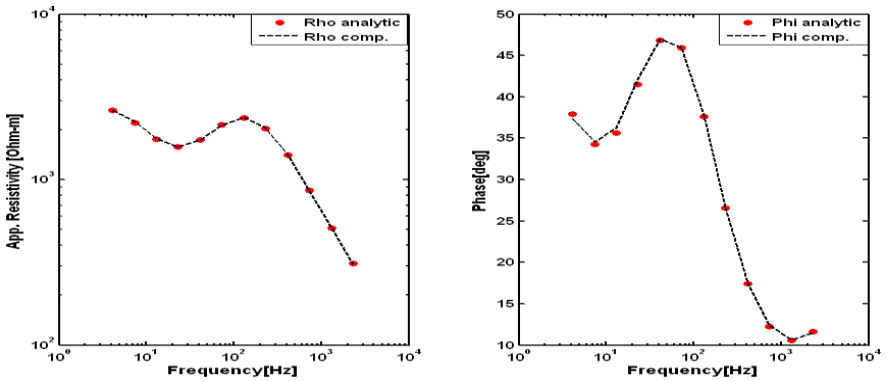

Figure 4: AMT sounding curves of the MT Inversion with Rhoplus of analytic data (Rho & Phi) (Parker and Booker 1996).

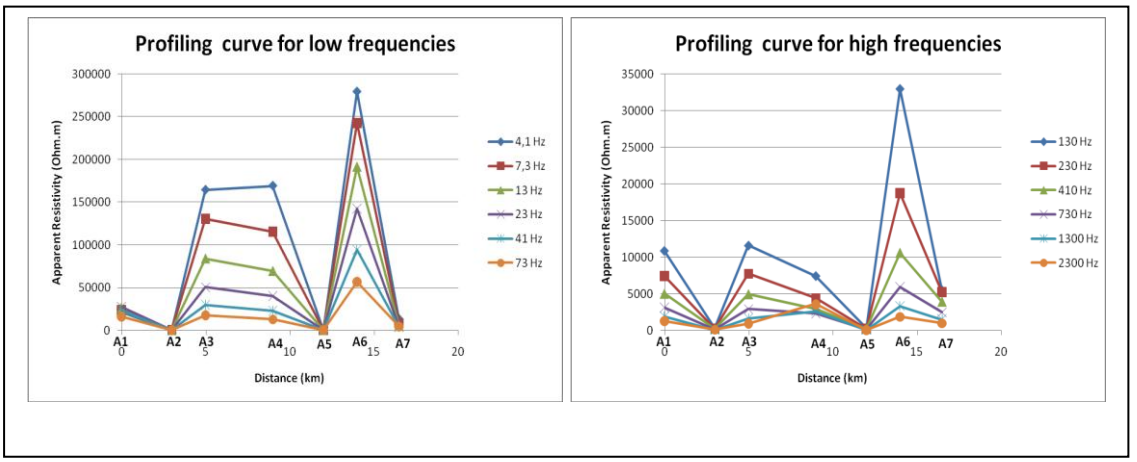

Figure 5: Profiling curves

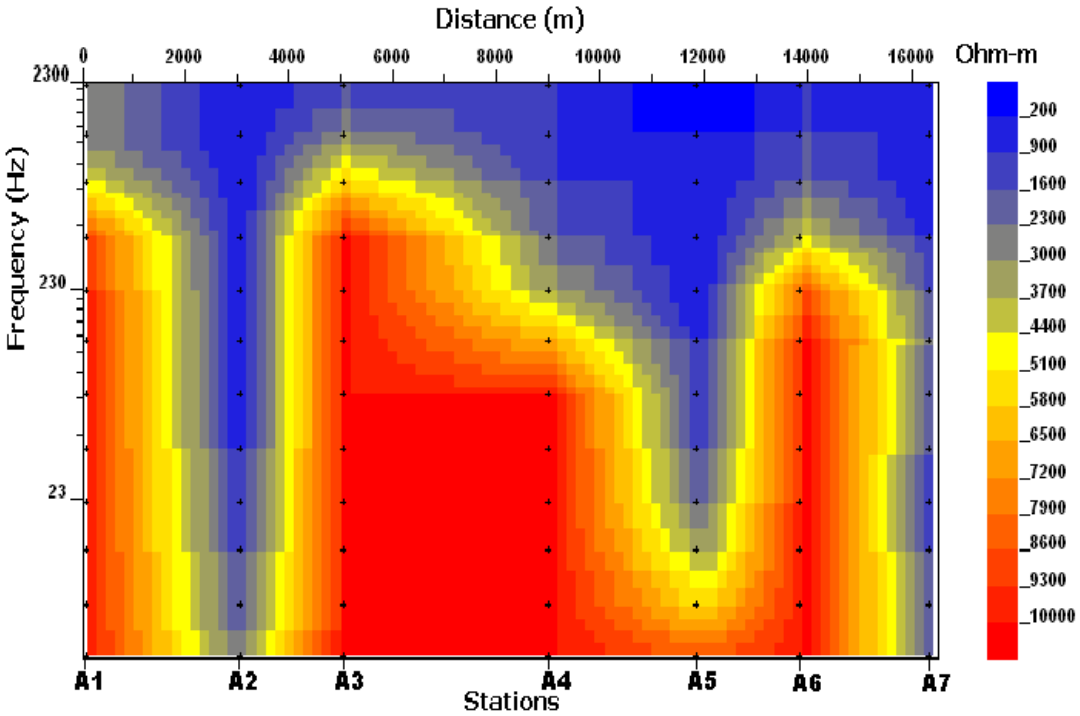

Figure 6: Pseudosections of resistivity

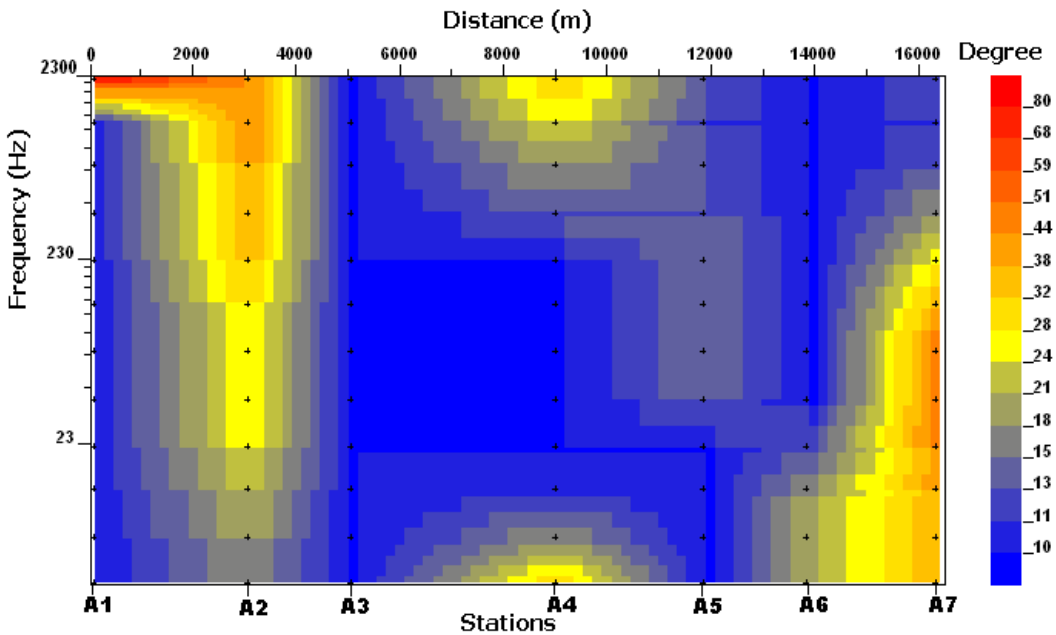

Figure 7: Pseudosections of phase

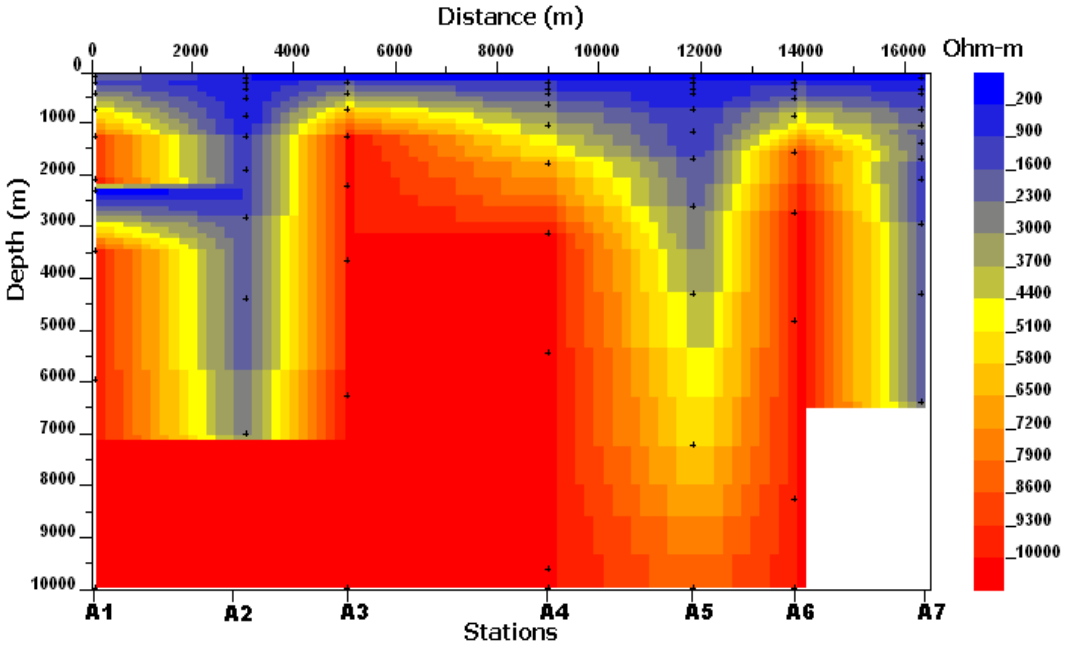

(a) : 2-D Resistivity section in mean depth (1km to 10 km)

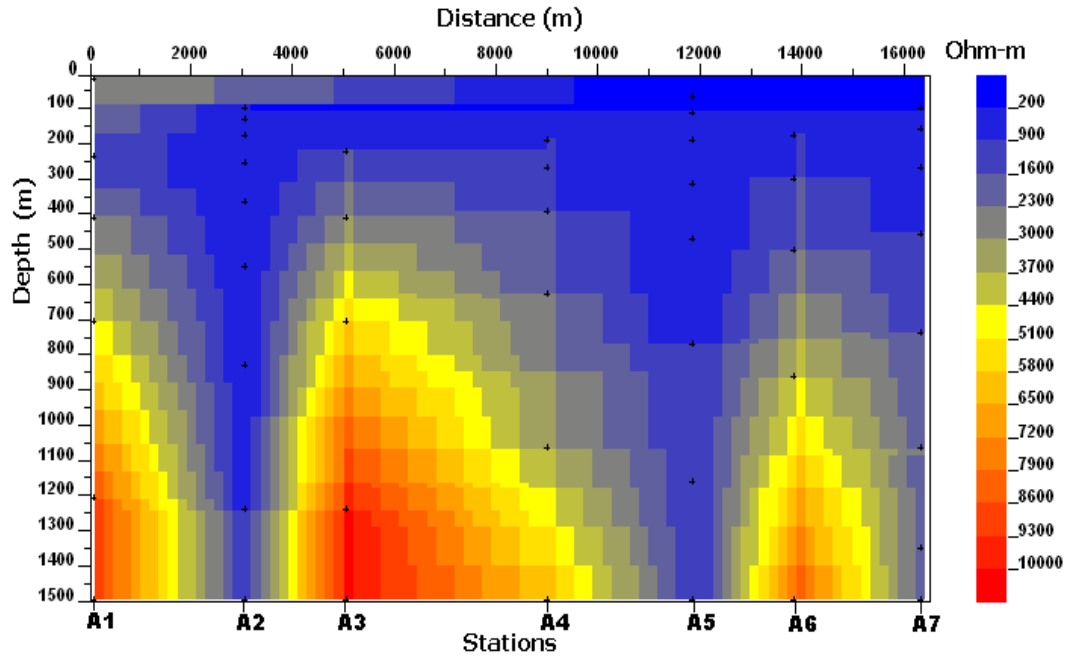

(b) : 2-D Resistivity section near surface (0 to 1 km)

Figure 8: 2-D Resistivity section: (a) in mean depth; (b) near surface

4.2 The Depth Investigation

The resistive-meter ECA 540-0, used in the data collection, do not permit us to have the depth of investigation directly. The skin effect δ is determined by the relation $\delta = 503\left(\frac{\rho_a}{F}\right)^{1/2}$ where ρ_a and F are the apparent resistivity and the frequency respectively (Manguelle-Dicoum et al, 1993). The skin effect δ is in meters. The depth of investigation P is half of the skin effect (Fauchard et al, 2004). The depth of investigation enables us to have 2-D Resistivity or geoelectrical section.

5 Results

5.1 Description of Profile

The profile (Fig. 1) cuts across the parallel 4°30'N and comprises seven (07) stations of measurement (Table 1). This profile oriented SN, is situated in the region crossing over the neoproterozoic series which comprised essentially the gneisses and migmatites of the mobile zone and strips of quartzites of specified Precambrian **(**Mvondo et al, 2007a) (Fig. 2b) or the younger metasediments and the Calco-Alkaline orthogneisses (Bisso et al, 2004). The area of investigation is consequently located on the line of Sanaga fault oriented SSW-NNE which is composed of recurrent faulting **(**Ngnotue et al, 2000). In this region, the metamorphism reaches a maximum in the Yaoundé region (granulites and migmatites), which then decrease to the north (Ngnotue et al, 2000).

5.2 Profiling Curves

The profiling curves (Fig. 5) show that the subsurface around A_1, between A_3 and A_4 and around A_6 is very resistive. It is characterized by the high gradient of resistivity relative to all frequencies. Around stations A_2 and A_5 one notes a sudden change of the profile lines for all frequencies. This behaviour around stations A_2 or A_5 characterize the presence of discontinuities about these stations (Bisso et al, 2004). These discontinuities are the conductive anomalies because the profile traverses a resistive region (Ballestreci et al, 1983; Manguelle-Dicoum et al, 1993). While, between A_6 and A_7 or around A_7, the profiling curves change suddenly. Indeed the gradient of resistivity falls abruptly between A_6 and A_7. These observations suggest the presence of conductive anomaly between these stations or around A_7 (Manguelle-Dicoum et al, 1993). The anomalies of A_2, A_5 and between A_6 and A_7 or around A_7 could be faults, fracture or the contact between two blocks of different lithology (Ballestreci et al, 1983; Bisso et al, 2004).

5.3 Pseudosections of Resistivity

The resistivity pseudosection (Fig. 6) below 410 Hz shows three high resistive zones (Rho>9000 Ω.m); which are the regions between A_3 and A_4, then around stations A_1 and A_6. Above 410 Hz, the resistivity falls (Rho<3000 Ω.m) for all stations. This resistivity decreases when the frequency increases. Around the stations A_2, A_5 and A_7, the pseudosections are sub-vertical and the resistivity is very small (Rho≤900 Ω.m) for all

frequencies. These observations suggest the presence of discontinuities around these stations. These discontinuities are the conductive anomalies because the profile crosses over a resistive subsoil (Rho>9000 Ω.m) (Ballestreci et al, 1983; Manguelle-Dicoum et al, 1993; Bisso et al, 2004). Below 410 Hz and above 410 Hz, the constrast is very small in regions situated between A_3 and A_4, A_1 and around A_6. Thus, the properties of geological structures in these are nearly similar on the one hand below 410 Hz, on the other hand above 410 Hz. These results are in accordance with those from profiling curves and particularly put in evidence that in depth (below 410 Hz), the subsoil is very resistive and near the surface (above 410 Hz), the subsoil is covered by the nearly conductive structures. It also specifies that the discontinuity localised between A_6 and A_7 is situated close to A_7 and extends further in depth.

5.4 Pseudosections of Phase

Following the AMT profile (Fig. 7) and around of the station A_2, pseudosections of phase are nearly vertical. At 2300 Hz, the phase is around 51°. These values decrease slightly when the frequency increases. Around stations A_1 and A_3, situated near A_2, the phase is very small (Phi<13°). These observations characterize on the one hand the presence of the discontinuity around the station A_2 covered by conductive structures, on the other hand a transition from conductive to more resistive structures (A_1 & A_3) (Ranganayaki, 1984; Jones et al, 1988). Around A_4, the phase (Phi≥21°) increases with the frequency above 410 Hz and below this frequency, the phase decrease until 23 Hz (Phi≤10°). From 23 Hz the phase increases again. Around A_5, the pseudosections are nearly vertical and the phase stays below 18° until 23 Hz, and then stays below 11° for small frequencies (F≤13 Hz). At the station A_6, the phase is very small (Phi≤10°) but from 23 Hz, the phase increases sligthly with small frequencies. At the station A_7 the phase is around 44° and the pseudosections are nearly vertical below 710 Hz. Above this frequency, the phase is small (Phi≤11°). These obsevations show on the one hand the presence of resistive structures around stations A_3, A_4 and A_6 limited by conductive structures around stations A_5 (above 23 Hz) and A_4 (above 410 Hz and below 23 Hz), on the other hand the presence of the discontinuity around A_5 (Ranganayaki, 1984; Jones et al, 1988). These observations also show the presence of conductive structures around A_7 and a discontinuity around this station limited in the hight frequencies by 710 Hz. These observations suggest a conductive anomaly in this area (Ranganayaki, 1984; Jones et al, 1988). These observations along the AMT profile confirm results of the profiling curve and the pseudo-section of resistivity.

5.5 2-D Resistivity Section

The Fig. 8a represents the geoelectrical section model or 2-D resistivity model. This figure shows that discontinuities around A_2, A_5 and A_7 extend to about 7000 m, 5500 and 6500 m in depth respectively. These discontinuities are characterized by nearly vertical pseudosections and small resistivities (Rho≤900 Ω.m) for all frequencies (Ranganayaki 1984; Manguelle-Dicoum et al, 1993, Bisso et al, 2004). But discontinuities around A_5 and A_7 seem to continue in depth because the investigation depths of the last frequency (4.1 Hz) limit the progression of waves in depth. This remark is justified by the very clear horizontal separation line between 7000 m and 8000 m around A_2 and absence of colours after 7000 m in depth around A_7 (Ranganayaki, 1984; Manguelle-Dicoum et al 1993;

Bisso et al 2004). The colour constrast of 2D-Resistivity model (Fig. 8b) assumes that the subsurface structure around stations A_1, A_3, A_4 and A_6 are models of four layers and A_2, A_5 and A_7 are models of three layers (Manguelle-Dicoum et al, 1993; Bisso et al, 2004). For the first three stations, the resistivity decreases between the first and the second layers but the thickness is small (Depth<100m) for the first layer. After the second layer, the resistivity increases with the depth. For the rest of the stations, the resistivity increases in depth from the first layer and this thickness is considerable (Depth>400 m). The last layer is very resistive (Rho>8000 Ω.m. Between A_1 and A_2, the 2-D Resistivy model (Fig. 8a) shows a lateral discontinuity characterized by the presence of a conductive structure ((Rho<900 Ω.m) between resistive structures (Rho>9000 Ω.m) (2300 m<Depth<3000 m) (Ranganayaki, 1984; Manguelle-Dicoum et al, 1993; Bisso et al, 2004). These observations along the AMT profile confirm on the one hand results of the profiling curve, pseudosections of resistivity and pseudosections of phase, and on the other hand bring to view the presence of lateral discontinuity or lateral conductive anomaly between A_1 and A_2.

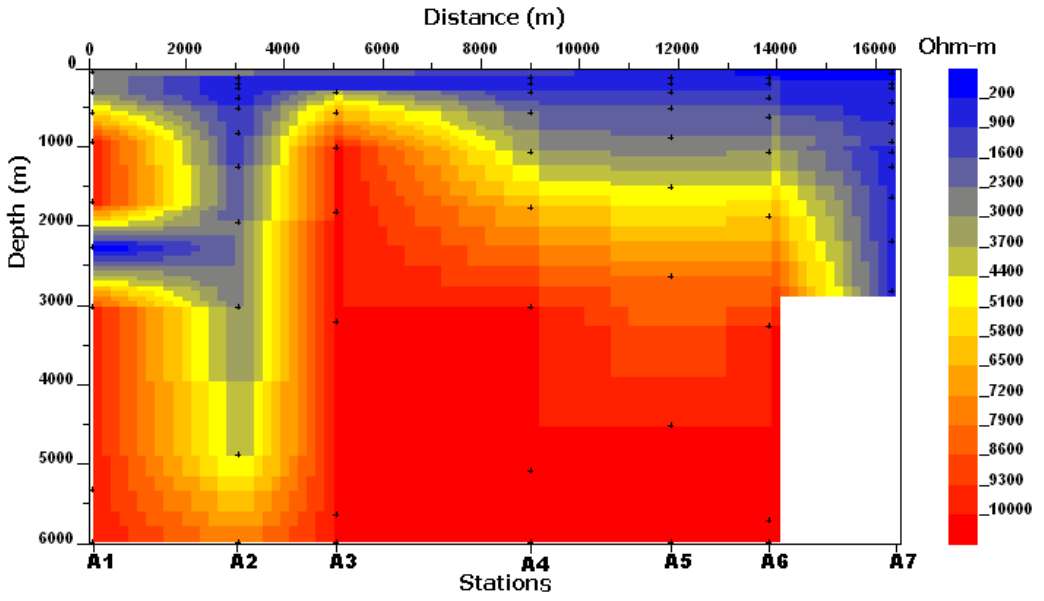

Figure 9: 2-D Resistivity section following the telluric line N-S

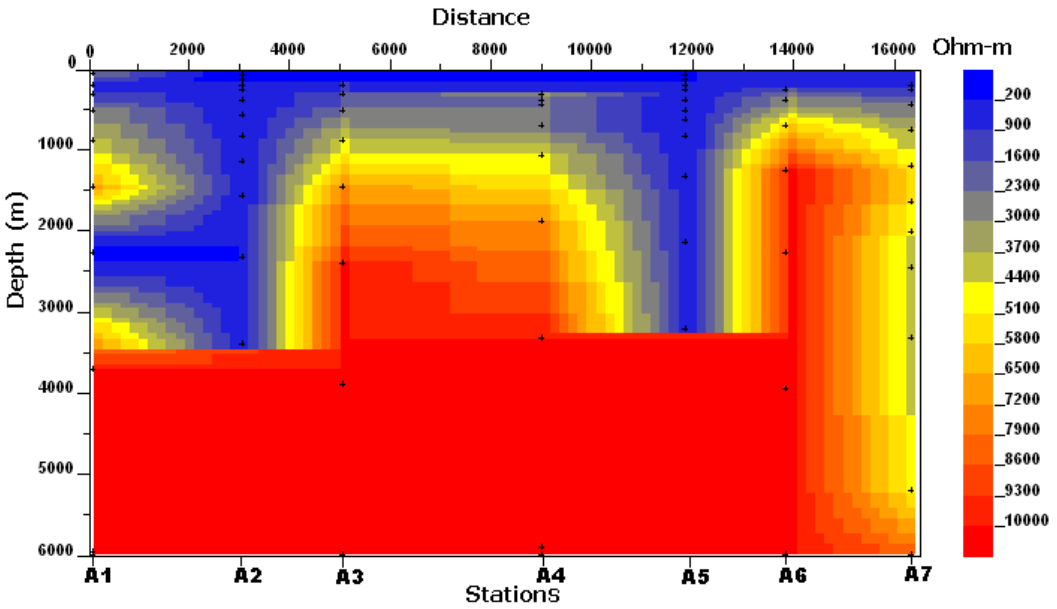

Figure 10 : 2-D Resistivity section following the telluric line E-W

6 Discussion

The Analysis of profiling curves, the pseudosections (resistivity and phase) and the 2D-Resistivity (geoelectrical section) reveal three discontinuity zones around the stations A_2, A_5 and A_7 (Figures 5, 6, 7 and 8a). These analyses show that the discontinuity about A_2 extends to below 6000 m while that about A_7 extends to above 6000 m (Fig. 8a). These analyses suggest that the discontinuities about A_2 and A_7 are major while that of A_5 is minor. It also suggests that these discontinuities or conductive anomalies are the faults, fractures or the contact between two blocks of different lithology (Ballestreci et al, 1983; Ranganayaki, 1984; Manguelle-Dicoum et al, 1993; Bisso et al, 2004). However, the particular analysis of 2-D Resistivity (Fig. 8a) shows except for discontinuities at A_2, A_5 and A_7, the presence of lateral discontinuity between A_1 and A_2 and situated below 3000 m from the surface (Manguelle-Dicoum et al, 1993). So to say, the 2-D Resistivity gives more information than apparent resistivity pseudosections or apparent phase pseudosections. Indeed it permits the localization of anomalies and the cartography of structures of the subsurface in depth (Ranganayaki, 1984). At the end of these analyses, one suggests that discontinuities or conductive anomalies around A_2 and A_7 are the faults while those around A_5 and between A_1 and A_2 are fractures (Ballestreci et al, 1983; Manguelle-Dicoum et al 1993; Bisso et al, 2004). The observation of 2-D Resistivity models following EW and SN telluric lines (Fig. 9 and 10), shows that only the discontinuity around A_2 is observable in the two directions. This major discontinuity (Manguelle-Dicoum et al, 1993; Bisso et al, 2004), occupy an intermediary position between the directions E-W and N-S. The course of Sanaga at the proximity of the Monatélé division which is the epicentre of the February 2005 earthquake in Monatélé and Northern areas of Yaoundé, follow an intermediary position between the directions E-W and N-S. This course of Sanaga seems to follow the Sanaga fault oriented SSW-NNE

(Dumont, 1986; Bisso et al, 2004). However the study area is consequently located on the line of Sanaga fault oriented SSW-NNE which is composed of recurrent faulting **(**Ngnotue et al, 200; Dumont, 1986). The position of the station A_2 at the right side of the Atlantic and near the Sanaga river let to suggestion that the discontinuity around A_2 would be the Sanaga fault which seems to follow the course of Sanaga (Bisso et al, 2004). This major fault, secant to a lateral fracture, is marked by a Biakoa-Goura fault network secant to the Sanaga fault characterized by discontinuities around A_5 and A_7. These results confirm the anterior geophysical studies and show that the fault network, secant to the Sanaga fault, belongs to the tectonic accident network (Dumont, 1986; Bisso et al, 2004). These results also correspond to the Pan African tectonic movement (Ngnotue et al, 2000).

The combination of the 2-D Resistivity and the pseudosections (resistivity and phase) with the standard table of resistivity range for rocks (Telford et al 1990; Parasnis, 1997) permits to suggest that the surface of the study area is covered by an alluvial deposits layer near the Sanaga river (stations A_1, A_2 and A_3) (Fig. 8b) and a conductive sedimentary layer essentially lateritic (Fig. 8a) on the northern part of the profile. But this combination also permits to suggest on the one hand that the second layer lies on structures constituted essentially of metamorphic quartzite, and on the other hand, on the basement constituted essentially of gneisses and migmatites. These results correlated with the geological observations, confirm the presence of the quartzite, gneisses and migmatites in the study area (Ngnotue et al, 2000; Bisso et al, 2004; Mvondo et al, 2007a).

The combination of the audiomagnetotellurics method (Cagniard 1953; Vozoff 1972 and 1990) and the MT inversion with Rhoplus (Parker and Booker, 1996) has led to put in evidence three discontinuities following the depth and a lateral discontinuity: the Sanaga fault communicating with the lateral discontinuity and oriented following the course of the Sanaga, and the Biakoa-Goura fault network characterised by the faults across Biakoa and Talba. These results permit us to say that the Monatele-Sa'a area is a seismic zone and the tectonic node relaxation of the Biakoa-Goura seems to be the origin of the February 2005 earthquake in Monatélé and Northern areas of Yaoundé. This combination has also permit to characterize the subsurface of the study area where the composition is mainly quartzite, migmatite and gneissic.

7 Conclusion

The combination of a geophysical investigation by audiomagnetotellurics method (Cagniard 1953; Vozoff 1972 and 1990), the MT inversion with Rhoplus (Parker and Booker, 1996) and the 2-D inversion has enabled us to contribute significantly to the understanding of the underground structure of the Monatélé-Sa'a zone. Indeed this zone is characterized by a major fault or Sanaga fault oriented SSW-NNE following the course of the Sanaga Elang III area, and the Biakoa-Goura II fault network characterised by the fault series traversing Biakoa and Talba. These faults make the Monatélé-Sa'a area a seismic zone that the tectonic node relaxation was the origin of the February 2005 earthquake in Monatélé and Northern areas of Yaoundé. This combination has also permitted to show that the characterised subsurface of the study area firstly, is covered in surface by alluvial deposits and the conductive sedimentary layers and secondly, it lies on quartzite, gneissic and migmatite structures. Furthermore, these results which correspond

to the tectonic movement of the area permit us to show on the one hand that the audiomagnetotellurics method is a reliable method in the imaging of subsurfaces, and on the other hand the 2D inversion (Parker and Booker, 1996) combined with a good knowledge of geology has given a good understanding of the Monatele earthquake.

References

[1] Ballestreci, R., Nougier, J. and Benderitter, Y. (1983). Existence and Interpreting of Electrically Conducting Zone within the Plateau Basalts Kerguelen Islands (T.A.A.F.). *C. R. Acad. Sc. Paris* II, **296**, 833-838.

[2] Bisso, D., Manguelle-Dicoum, E., Ndougsa-Mbarga, T., Tabod, C. T., Njandjock, N. P., Njingti, N., Tadjou, J. M. and Essono, J. (2004). Geophysical Determination of the Sanaga Fault using Audio-magnetotelluric soundings in the Ebedda region, Cameroon. *SEGMITE International,* **1**(1), 31-34.

[3] Cagniard, L. (1953). Basic theory of the magneto telluric method of geophysical prospecting. *Geophysics*, **18**, 605-635.

[4] Cornacchia, M. and Dars, R. (1983). Un trait structural majeur du continent africain. Les linéaments centrafricains du Cameroun au golfe d'Aden. *Bull. Soc. Geol. Fr.*, **25**, 101-109

[5] Dumont, J. F. (1986). Identification par télédétection de l'accident de la Sanaga (Cameroun). Sa position dans le contexte des grands accidents d'Afrique Centrale et de la limite nord du craton congolais. *Géodynamique,* **2**(1), 55-68.

[6] Guérin, R., Tabbach, A., Benderitter, Y., Andrieux, A. (1994). Invariant for correcting field polarization effect in MTVLF resistivity mapping. *Journal of Applied Geophysics*, **32**, 375-383.

[7] Jones, A. G., Kurtz, R. D., Oldenburg, D. W., Boerner, D. E. and Ellis, R. (1988). Magneto-telluric observations along the Lithoprobe southeastern Canadian Cordilleran transect. *Geophysical Research Letters*, **15**(7), 677-680.

[8] Jones, A. G. (1988). Static shift of magnetotelluric data and its removal in a sedimentary basin environment. *Geophysics*, **53**(7), 967-978.

[9] Jones, A. G. and Garcia, X. (2003). Case History Okak Bay AMT data-set case study: Lessons in dimensionality and scale. *Geophysics*, **68**(1), 70-91.

[10] Manguelle-Dicoum, E., Bokossah, A. S. and Kwende-Mbanwi, T. E. (1992). Geophysical evidence for a major Precambrian schist-granite boundary in Southern Cameroon. *Tectonophysics*, **205**, 43-446.

[11] Manguelle-Dicoum, E., Nouayou, A. S., Bokossah, A. S. and Kwende-Mbanwi, T. E. (1993). Audiomagnetotelluric soundings on the basement-sedimentary transition zone around the Eastern margin of the Douala Basin in Cameroun. *J. Afr. Earth Sci.*, **17**(4), 487-496.

[12] Meying, A., Ndougsa-Mbarga, T. and Manguelle-Dicoum, E. (2009). Evidence of fractures from the image of the subsurface in the Akonolinga-Ayos area (Cameroon) by combining the Classical and the Bostick approaches in the interpretation of audio-magnetotelluric data. *Journal of Geology and Mining Research,* **1**(8), 159-171.

[13] Mvondo, H., Owona, S., Mvondo-Ondoa, J. and Essono, J. (2007). The tectonic evolution of the Yaoundé segment of the Neoproterozoic Central African Orogenic Belt in southern Cameroun. *Can. J. Earth Sci*., **44**, 433-444.

[14] Ngnotue, T., Nzenti, J.P., Barbey, P. and Tchoua, F.M. (2000). The Ntui-Betamba high grade gneisses: a northwest extension of the Pan-African Yaoundé gneisses in Cameroon *J. Afr. Earth Sci.,* **31**, 369-381.

[15] Nzenti, J. P., Barbey, P., Macaudière, J. and Soba, D. (1988). Origin and Evolution of the Precambrian high grade Yaoundé gneiss (Cameroon). *Precambrian Res.,* **38**, 91-109.

[16] Parasnis, D. S. (1997). Principles of Applied Geophysics. *5th edition Chapman and Hall, London, England*, 400 p.

[17] Parker, R. L. and Booker, J. R. (1996). Optimal one-dimensional inversion and bounding of magnetotellurics apparent resistitvity and phase measurements. *Physics of the Earth and Planetary Interiors*, 269-282

[18] Penaye, J., Toteu, S. F., Van Schmus, W. R. and Nzenti, J. P. (1993). U-Pb and Sm-Nd preliminary geochronologic data on the Yaoundé Series, Cameroun: re-interpretation of the granulitic rocks as the suture of collision in the Central African Belt. *C. R. Acd. Sci. Paris* II, **317**, 789-794.

[19] Pham, V. N., Boyer, D. and Chouteau, M. (1978). Mapping of apparent pseudoresistivity by combination of Telluric-Telluric and magnetotelluric profiling. *Geophysical prospecting*, **26**, 218-246.

[20] Raganayaki, R .P. (1984). An interpretive analysis of magnetotelluric data. *Geophysics*, **49**, 1730-1748.

[21] Telford, W. M., Geldart, L. P., Sheriff, R. E., Keys, D. A. (1990). *Applied geophysics. 2th edition Cambridge University press, Cambridge, GB*, 770p.

[22] Vozoff, K. (1972). The Magnetotellurics method in the exploration of sedimentary basins. *Geophysics,* **37**(1), 98-141.

[23] Vozoff, K. (1990). Magnetotelluric principles and practice. *Proc. Indian Acad. Sci.,* **99**(4), 441-471.